Renormalized-Free-Atom Model and the Electron Momentum Distribution in Vanadium

K.-F. Berggren
University of Linköping, Department of Physics, S-581 83 Linköping, Sweden
(Received 6 March 1972)

Recent measurements of the Compton profile of polycrystalline vanadium have been interpreted by means of a renormalized-free-atom model. The electronic configuration has been varied, and it has been found that the configuration in vanadium must be close to $3d^4 4s^1$ in atomic notations, in agreement with earlier experience.

I. INTRODUCTION

During the last few years there has been a rapidly increasing interest in inelastically scattered (Compton) x rays.[1] With certain simplifying assumptions, the so-called impulse approximation, the spectrum of the inelastically scattered x rays—the Compton profile—is directly related to the electron momentum distribution of the scattering system. Compton-scattering experiments are particularly sensitive to the momentum distribution of outer weakly bound electrons, and therefore provide an interesting way of testing the wave functions used to describe, for example, the band electrons in a metal. Measurements on a polycrystalline sample yield the Compton profile, defined as

$$J(q) = \int_q^\infty dp\, p \langle \rho(\vec{p}) \rangle, \tag{1}$$

where $\langle \rho(\vec{p}) \rangle$ is the spherical average of the electron momentum distribution $\rho(\vec{p})$. For a single orbital $\chi(\vec{r})$ the momentum distribution is given by

$$\rho(\vec{p}) = |\chi(\vec{p})|^2, \tag{2}$$

where

$$\chi(\vec{p}) = (2\pi)^{-3/2} \int d\vec{r}\, e^{-i\vec{p}\cdot\vec{r}} \chi(\vec{r}) \tag{3}$$

defines the momentum transform.[2] Given a certain wave function for a system one may evaluate the corresponding momentum distribution and a theoretical Compton profile. A comparison of the experimental and theoretical profiles would then give an estimate of the reliability of the assumed electronic configuration and wave function.

Most Compton experiments on itinerant-electron systems have been centered on the simple metals. Measurements have been performed successfully on Li,[3–5] Na,[3] Be,[3] Mg,[3,6] and Al.[3,7] With a few exceptions[4,8,9] the data have so far been interpreted by means of the free-electron model for the conduction electrons and free-atom wave functions for the core electrons. Measurements on the potentially more interesting, but also more difficult transition metals have recently begun. Isotropic profiles are now available for Sc,[10] Ti,[11] V,[12] and Fe.[13,14] The results have again been interpreted in terms of either the free-electron model or free-atom wave functions. None of these models is satisfactory for a transition metal, and evidently there is a need for a somewhat better description of the electronic structure in analyzing the Compton data. Particularly in the low-momentum region, which is most sensitive to the shape of the outermost-electron wave functions, there are significant deviations from free-atom behavior. In principle one knows how to obtain a more accurate description. From a complete band-structure calculation by means of, e.g., the Korringa-Kohn-Rostoker (KKR) method the wave functions $\psi_{\vec{k}}(\vec{r})$ and hence the momentum transforms $\psi_{\vec{k}}(\vec{p})$ could be extracted. The momentum density is then obtained as

$$\rho(\vec{p}) = \sum_{\vec{k}} |\psi_k(\vec{p})|^2, \tag{4}$$

in which the summation includes all the states below the Fermi surface. An evaluation of the Compton profile in this ambitious way would apparently be rather tedious. Although work on iron along these lines is in progress,[15] we believe it worthwhile to try a simpler approach. For this purpose we will make use of an elementary model, namely, the "renormalized-free-atom"(RFA) model,[16–18] which makes a reasonable compromise between a proper band-structure calculation and a free-atom description. In a simple way this approach brings in the fact that the atom is not free, but confined to a particular cell in a solid. In this paper we will investigate the case of polycrystalline vanadium, and we find that the model is capable of predicting a qualitatively satisfactory Compton profile. Hopefully the model will serve as a good starting point for more sophisticated treatments including band-structure and intra-atomic d-d correlation effects. Finally, our calculation serves as a test of the RFA model itself.

In Sec. II we describe the RFA model and derive the formulas for the isotropic Compton profile. In Sec. III we present numerical results for polycrystalline vanadium, and compare them with experiment. A discussion of the result is also given in Sec. III. Some useful formulas for the evaluation of the momentum transforms of truncated Slater-type orbitals are given in the Appendix. The emphasis of the present work is on gross

properties rather than details.

II. RENORMALIZED ATOMS AND COMPTON PROFILE

The renormalized-atom approach was first used by Chodorow,[19] and extended by Segall[20] for Cu. In this scheme one utilizes the free-atom Hartree-Fock wave functions, truncates them at R_0 of the Wigner-Seitz sphere, and renormalizes them within this sphere thereby preserving charge neutrality. In this way the solid is constructed from individual atoms, which are prepared in approximately the form in which they actually enter the solid before placing them together. Watson and co-workers[16-18] have recently shown that the renormalized-atom model yields quantitatively correct estimates of important band-structure characteristics as well as an explanation of the cohesion in the transition-metal series. For example, the renormalized-atom energies ϵ_d and ϵ_Γ provide an excellent estimate of the energetic position of the center of gravity of the d band and the conduction-band minimum, respectively. In the following considerations we will disregard hybridization effects.

A. s Electrons

When a free atom is placed in a solid it is known that the core states, which have exceedingly small amplitudes at R_0, are practically unchanged. Apart from a normalization factor the crystal wave function for the conduction-band minimum and the corresponding free-atom wave function are then expected to be quite similar in the core region. This is because in the region the wiggles in the two wave functions are merely a consequence of the orthogonality to the core states, which for most purposes could be considered identically the same for the crystal and the atom. Figure 1 shows the radial part $R_{4s}(r)$ of Clementi's[21] free-4s-atom wave function for vanadium, computed within the Hartree-Fock scheme and with the electronic configuration $3d^3 4s^2$. The same figure also shows the 4s function truncated at the Wigner-Seitz radius $R_0 = 2.82$ a.u. and renormalized to one within the sphere. Beyond its last maximum the renormalized 4s function decreases slowly towards the cell boundary. The slow variation of the associated charge density in the outer region of the cell is apparently in accordance with the idea of almost free conduction electrons in vanadium. The over-all shape of the renormalized function is therefore quite reasonable. The wave function satisfies, however, only approximately the Wigner-Seitz boundary condition $R'_{4s}(R_0) = 0$. For this reason we have also tried an improved version of the 4s function as indicated in Fig. 1. Beyond its last maximum at $R_{\max}$, the function is set equal to a constant $R_{4s}(R_{\max})$ and properly renormalized. The boundary condition is then satisfied in a simple way, but it was noticed subsequently that this improvement led to numerically insignificant changes in the computed Compton profile. This may be taken as an indication that the violation of the Wigner-Seitz boundary condition in the renormalized-atom approach is not very severe. For this reason the RFA function in Fig. 1 is a good representation of the true crystal wave function at $\vec{k} = 0$, and the two functions are almost identical, not only in shape but also in magnitude, within the core region.[22]

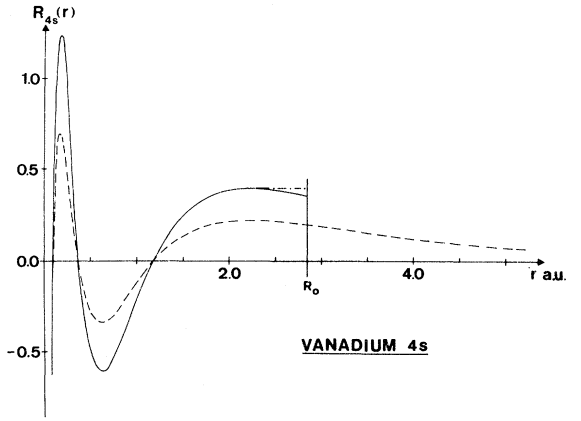

FIG. 1. Free-atom 4s wave function for vanadium (dashed curve) and the same function truncated at the Wigner-Seitz radius and renormalized to one within the sphere (full curve). The horizontal line indicates a simple way of satisfying the Wigner-Seitz boundary condition, as discussed in the text.

B. Momentum Transform and Compton Profile for s Electrons

We will now proceed to the evaluation of the expression for the isotropic Compton profile for the (unhybridized) 4s band. For this purpose we have to consider the momentum transform of a Bloch function, which for cubic structures is given by

$$\psi_{\vec{k}}(\vec{p}) = N\,\delta_{\vec{p}-\vec{k},\vec{K}_n}\,\psi^c_{\vec{k}}(\vec{p}). \tag{5}$$

In this equation N is the total number of atoms, and the transform $\psi^c_{\vec{k}}(\vec{p})$ is defined as

$$\psi^c_{\vec{k}}(\vec{p}) = (2\pi)^{-3/2} \int_{\Omega_0} d\vec{r}\, e^{-i\vec{p}\cdot\vec{r}}\,\psi_{\vec{k}}(\vec{r}), \tag{6}$$

where region of integration in Eq. (6) is over a Wigner-Seitz polyhedron. In the conventional cell approximation

$$\psi_{\vec{k}}(\vec{r}) = e^{i\vec{k}\cdot\vec{r}}\,\psi_{\vec{k}=0}(\vec{r}), \tag{7}$$

the transform in Eq. (6) simplifies to

$$\psi^c_{\vec{k}}(\vec{p}) = \psi^c_0(\vec{K}_n), \tag{8}$$

with $\vec{p} - \vec{k} = \vec{K}_n$. Some caution must be exercised in evaluating $\psi^c_0(\vec{K}_n)$. The region of integration must not immediately be replaced by the Wigner-Seitz sphere. To preserve normalization of $\psi_{\vec{k}}(\vec{p})$ in Eq. (5) we write

$$\psi_{\vec{k}}^{c}(\vec{p}) = (2\pi)^{-3/2} \int_{\Omega_0} d\vec{r}\, e^{-i\vec{K}_n\cdot\vec{r}} \cdot [\psi_0(\vec{r}) - \psi_0(R_0)] + (2\pi)^{-3/2}\Omega_0\, \delta_{\vec{K}_n,0}\, \psi_0(R_0). \quad (9)$$

The spherical approximation may now be performed for *this* integral.[23]

The momentum density per atom is given by

$$\rho(\vec{p}) = 2\sum_{\vec{k}} \delta_{\vec{p}-\vec{k},\vec{K}_n} |\psi_0^c(K_n)|^2, \quad (10)$$

where $\vec{k}$ runs over all occupied states and the factor of two comes from summation over spin. If we assume a spherical population of s states the spherical average of $\rho(\vec{p})$ is easily taken. The Kronecker δ in Eq. (10) is replaced by the condition $|\vec{K}_n - \vec{p}| \leq p_F$ and we obtain (see Fig. 2)

$$\langle\rho(\vec{p})\rangle = 2\sum_{n=0}^{\infty} F_n(p) |\psi_0^c(K_n)|^2. \quad (11a)$$

For $n \neq 0$ we have

$$F_n(p) = N_n[p_F^2 - (K_n - p)^2]/4K_n p, \quad (11b)$$

if $p \in (K_n - p_F, K_n + p_F)$, and zero otherwise. N_n is the number of reciprocal lattice points in the nth shell, and p_F the Fermi momentum for the s electrons. For $n = 0$ we have

$$F_0(p) = \begin{cases} 1, & p \leq p_F \\ 0, & p > p_F. \end{cases}$$

Elementary integration finally gives the expression for the isotropic Compton profile as

$$J_{4s}(q) = 4\pi\sum_{n=0}^{\infty} |\psi_0^c(K_n)|^2 G_n(q). \quad (12)$$

For $n \neq 0$ we have

$$G_n(q) = \begin{cases} 0, & q > K_n + p_F \\ \tilde{G}(q), & q \in (K_n - p_F, K_n + p_F) \\ \tilde{G}(K_n - p_F), & q < K_n - p_F \end{cases} \quad (13)$$

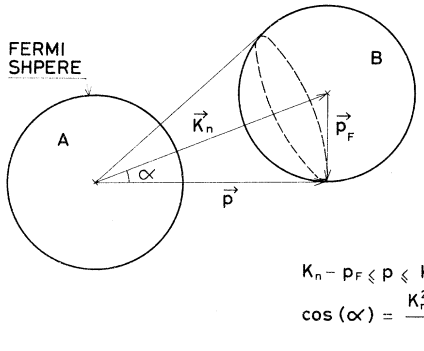

FIG. 2. Geometrical construction for taking the spherical average of the momentum density. In the Seitz approximation the momentum density within each sphere centered at $\vec{K}_n$ is equal to a constant $|\psi_0^c(K_n)|^2$, and zero outside. The integration is carried out over the surface segment of a sphere of radius p, which intersects the sphere B.

where the auxiliary function $\tilde{G}(x)$ is defined as

$$\tilde{G}_n(x) = N_n\{(p_F^2 - K_n^2)(K_n + p_F - x) - \tfrac{1}{3}[(K_n + p_F)^3 - x^3] + K_n[(K_n + p_F)^2 - x^2]\}/4K_n. \quad (14)$$

For $n = 0$ we have

$$G_0(q) = \tfrac{1}{2}(p_F^2 - q^2), \quad (15)$$

if $q \leq p_F$ and zero otherwise.

In the approximation that the $4s$ electrons form a uniform electron gas the Compton profile would be

$$J_{gas}(q) = [\Omega_0/(2\pi)^2](p_F^2 - q^2) \quad (16)$$

for $q \leq p_F$ and zero otherwise. Apart from a factor the Wigner-Seitz model predicts exactly the same profile for $q \leq p_F$. The higher terms in Eq. (12) reflect the variation of $\psi_0(r)$ within the Wigner-Seitz cell, and give rise to a tail in $J_{4s}(q)$ for $q > p_F$.

C. *d* Electrons

Clementi's[21] atomic $3d$ functions, which have been used in our calculations, are to 96% contained in the Wigner-Seitz sphere. This is in contrast to 31% for the $4s$ function. We may then conceive of the $3d$ electrons as forming a very narrow band. As we are looking for gross properties rather than details we will neglect all overlap (or renormalization), and consider the d electrons only in the extreme tight-binding approximation

$$\psi_{\vec{k}}(\vec{r}) = N^{-1/2}\sum_g e^{i\vec{k}\cdot\vec{R}_g}\, \chi_{3d}(\vec{r} - \vec{R}_g), \quad (17)$$

where $\chi_{3d}(\vec{r})$ is an atomic function centered at lattice point $\vec{R}_g$. For the momentum density per atom we then find

$$\rho_l(\vec{p}) = 2\,\frac{2l+1}{4\pi}\,|R_l(p)|^2 \sum_{\vec{k}} \delta_{\vec{p}-\vec{k},\vec{K}_n}, \quad (18)$$

where $\vec{k}$ runs over all occupied states, and

$$|R_l(p)|^2 = (2/\pi)\left|\int_0^{\infty} dr\, r^2 R_l(r) j_l(pr)\right|^2. \quad (19)$$

Equation (18) includes summation over spin. $R_l(r)$ is the normalized radial part of the wave function. For a completely filled zone one can always find a vector $\vec{K}_n$ such that the condition $\vec{p} - \vec{k} = \vec{K}_n$ is satisfied. Eq. (18) then simplifies to

$$\rho_l(\vec{p}) = 2[(2l+1)/4\pi]\,|R_l(p)|^2, \quad (20)$$

i.e., the momentum density of the isolated atom. This result is of course expected for closed-core shells.

For a partially filled zone, as for the d states in vanadium, the summation in Eq. (18) has to be performed. In the general case this is not easy. If we assume, however, a spherical occupation we obtain, in the same way as for the s electrons, the averaged momentum density

$$\langle \rho_l(\vec{p}) \rangle = [2(2l+1)/4\pi] |R_l(p)|^2 Q(p), \quad (21)$$

where

$$Q(p) = \sum_{n=0}^{\infty} F_n(p). \quad (22)$$

The functions $F_n(p)$ are the same as in Eqs. (11b) and (11c), but with p_F replaced with a "Fermi momentum" p_0 for the d electrons. The spherical approximation of the occupied region of the zone is not as drastic as it may look. The Bloch functions are assumed to be d like everywhere in the zone, and the function $Q(p)$ mainly serves to count the number of electrons in the band. The properly normalized profiles computed with the two expressions in Eqs. (20) and (21) have been found to be practically the same. Other choices of the occupied region would presumably lead to the same result since the $3d$ momentum density varies rather slowly with p. Within the extreme tight-binding scheme it is consequently a good approximation to use a superposition of the momentum densities of the free atoms also in the case of unfilled bands, as was done in Refs. 10–14.

III. RESULTS AND DISCUSSION

The Compton profile of polycrystalline vanadium has recently been measured by Paakari *et al.*[12] using 59.54-keV γ rays from an ^{241}Am source. The experimental data (before smoothing) are given in Figs. 3 and 4 for different values of p_z, where p_z is the component of the electron's initial momentum along the scattering vector. In the case of the vanadium measurements, $p_z \sim 0.9q$. The percentage error at some points are: 2.5% at $p_z = 0.0$; 3.5% at 1.5; 5.5% at 3.0; and 8% at 6.0.

In Sec. II we have discussed an elementary model for transition metals, consisting of a $4s$-band overlapping a narrow d-band. Hybridization effects were, however, not included. By means of the formulas derived in Sec. II we have calculated the Compton profile of polycrystalline vanadium. In these calculations we have used Clementi's[21] analytical Hartree-Fock wave functions, computed for the atomic configuration $3d^3 4s^2$. In order to determine the electronic structure of the vanadium metal, the s and d content have been varied until a reasonable agreement with experiment was obtained. In this way it was concluded that a configuration with one electron in the $4s$ band and four in the d band (or very close to that) gives the best fit to the measured points. A $3d^3 4s^2$ occupancy, for example, would give a completely unrealistic profile. The results of the numerical calculations are displayed in Figs. 3 and 4. Included are also the contributions from the electrons $1s^2 2s^2 2p^6 3s^2 3p^6$ as computed from Clementi's[21] wave functions. In view of the elementary model we have used the computed Compton profile is quite satisfactory. In particular, the deviations from a free-atom description at low momenta are well accounted for.

The $d^{n+1}s^1$ configuration derived above is consistent with most solid-state experience and has been found to yield successful and nearly self-consistent results for a number of transition metals. For example in the augmented-plane-wave calculations by Snow and Waber[24] the computed character of the occupied bands favors an occupancy nearer

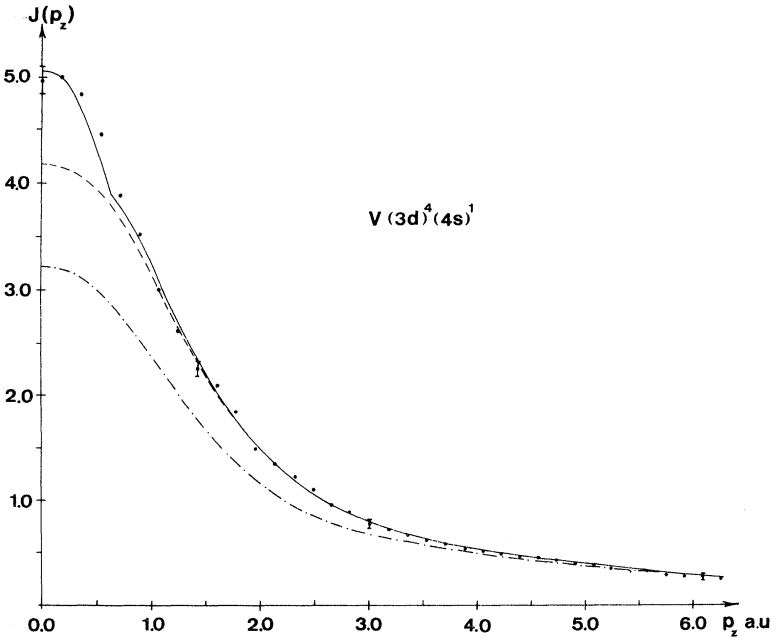

FIG. 3. Experimental and calculated Compton profiles of polycrystalline vanadium. The dots refer to experiments; the statistical error is indicated for some points. The solid curve is calculated from a superposition of free-atom core functions and a renormalized $4s$ atomic function. The electronic configuration is chosen as $1s^2 2s^2 2p^6 3s^2 3p^6 3d^4 4s^1$. The dashed curve is the Compton profile with the $4s^1$ contribution subtracted, and the dot-dashed curve with the $4s^1$ and $3d^4$ contributions subtracted.

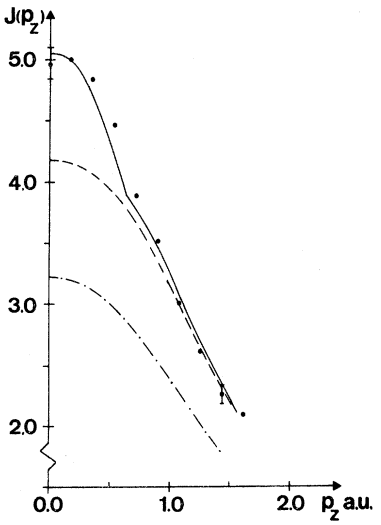

FIG. 4. Experimental and calculated Compton profiles at low momenta. The notations are the same as in Fig. 3.

to $3d^4 4s^1$ than $3d^3 4s^2$ for vanadium. Mattheiss[25] has also calculated the energy bands for vanadium using two different starting potentials generated from the atomic $3d^3 4s^2$ and $3d^4 4s^1$ configurations. The effect of the differences in these potentials is quite dramatic and reemphasizes the uncertainties inherent in band-structure calculations for transition metals, at least for those which are not self-consistent. With our promising results for the Compton profile a potential derived from the renormalized-atom wave function of this paper should therefore be useful in connection will full band-structure calculations on vanadium.

Our results for the renormalized-atom approach reconfirms the theoretical analysis of Paakari *et al.*[12] For $p_z \gtrsim 1$, the contribution to the Compton profile from the s band is almost negligible. With the remarks in Sec. IIC in mind the analysis in this region may therefore be based entirely on free-atom wave functions. In this way Paakari *et al.* found that the medium and high parts derive from four $3d$ electrons plus core.

In summary, the renormalized-atom approach as used in this paper has been shown to yield a quite satisfactory Compton profile for vanadium. There are, however, several apparent improvements to be made. It is known that the Compton profile is sensitive to electron-electron correlations. From electron-gas data[1,26] it is expected that the profile deriving from the $4s$ band, and which indeed is very free-electron-like, should be broadened by a few percent. The discontinuity at the Fermi surface would remain, but a high-momentum tail would be added. The inclusion of correlation effects in the $4s$ band would therefore bring us closer to experiment. On the basis of a strong interaction model for d bands in transition metals, Hubbard[27] has proposed the possibility of dramatic correlation effects for the d electrons. Although such interesting effects would presumably show up in Compton profile measurements on transition metals it is at present hard to evaluate them quantitatively. Because of these uncertainties about the d band we have refrained from computing correlation effects also in the s band. The present calculation could also be improved by including band-structure effects and hybridization. It is expected, however, that hybridization would lead to small changes in the isotropic Compton profile. In fact, if both the upper and lower hybridized bands are occupied, the effect is none, since hybridization has the character of a unitary transformation. If only the lower band is occupied, the effect is small, because the mixing of the s and d bands is effective only in a small region where these bands cross. Finally, the present work could be improved by using wave functions from a $3d^4 1s^1$ free-atom calculation. Unfortunately such wave functions are not available in the literature.

ACKNOWLEDGMENTS

The author is indebted to Dr. T. Paakkari, Dr. S. Manninen, Dr. O. Inkinen, and Dr. E. Liukkonen for communicating data for vanadium prior to publication. The correspondence with Dr. O. Inkinen has been particularly helpful.

APPENDIX

Clementi's[21] atomic wave functions are given as linear combinations of Slater-type orbitals $r^{n_i} e^{-\alpha_i r}$. Taking the momentum transform as defined in Eq. (6) integrals of the type

$$I_n(\alpha, p) = \int_0^R dr\, r^n e^{-\alpha r} \sin(pr)/p \tag{A1}$$

appear for s functions. By partial integrations we obtain the recurrence relation

$$(\alpha^2 + p^2) I_n = 2\alpha n I_{n-1} - n(n-1) I_{n-2} - R^n e^{-\alpha R}[(\alpha R - n)\, j_0(pR) + \cos(pR)]. \tag{A2}$$

The recurrence is started with

$$I_0 = \frac{1 - e^{-\alpha R}[\alpha R\, j_0(pR) + \cos(pR)]}{\alpha^2 + p^2} \tag{A3}$$

and $I_1 = -\partial I_0/\partial\alpha$. In the limit $R \to \infty$, Eq. (A2) reduces to the well-known recurrence formula for the transform of free Slater orbitals of s symmetry.

[1]For a recent review, see M. Cooper, Advan. Phys. 20, 453 (1971). This article contains a large number of references to experimental and theoretical works.

[2]Atomic units $m = e^2 = \hbar = 1$ are used throughout.

[3]W. C. Phillips and R. J. Weiss, Phys. Rev. 171, 790 (1968).

[4]M. Cooper, B. G. Williams, R. E. Borland, and J. R. A. Cooper, Phil. Mag. 22, 441 (1970).
[5]W. C. Phillips and R. J. Weiss, Phys. Rev. B 5, 755 (1972).
[6]R. J. Weiss, Phil. Mag. 24, 1477 (1971).
[7]J. Felsteiner, R. Fox, and S. Kahane, Solid State Commun. 9, 61 (1971).
[8]R. Currat, P. D. De Ciccio, and R. Kaplow, Phys. Rev. B 3, 243 (1971).
[9]B. I. Lundqvist and C. Lydén, Phys. Rev. B 4, 3360 (1971).
[10]S. Manninen, J. Phys. F 1, 60(L) (1971).
[11]R. J. Weiss, Phys. Rev. Letters 24, 883 (1970).
[12]T. Paakkari, S. Manninen, O. Inkinen, and E. Liukkonen, Phys. Rev. B 6, 351 (1972).
[13]M. Cooper and B. G. Williams, Phil. Mag. 17, 1079 (1968). This article contains exploratory measurements on Fe.
[14]J. Felsteiner, R. Fox, and S. Kahane, Solid State Commun. 9, 457 (1971).
[15]P. Mijnarends (private communication).
[16]R. E. Watson, H. Ehrenreich, and L. Hodges, Phys. Rev. Letters 24, 829 (1970).
[17]R. E. Watson and H. Ehrenreich, Comments Solid State Phys. III, 109 (1970).
[18]L. Hodges, R. E. Watson, and H. Ehrenreich, Phys. Rev. B 5, 3953 (1972).
[19]M. Chodorow, Phys. Rev. 55, 675 (1939).
[20]B. Segall, Phys. Rev. 125, 109 (1962).
[21]E. Clementi, IBM J. Res. Develop. 9, 2 (1965).
[22]The close resemblance between a renormalized 4s atom wave function and a crystal wave function was noticed in a self-consistent Wigner-Seitz calculation for Fe in equilibrium and compressed states. For expanded states the renormalized approach ceases to be a good approximation, since the truncated function is allowed to fall off too much with r. The shape of the two functions in the core region is still the same, but normalization effects lead to different amplitudes [K. - F. Berggren and A. Froman (unpublished)].
[23]S. Berko and J. S. Plaskett, Phys. Rev. 112, 1877 (1958).
[24]E. C. Snow and J. T. Waber, Acta Met. 17, 623 (1969).
[25]L. F. Mattheiss, Phys. Rev. 134, A970 (1964).
[26]E. Daniel and S. H. Vosko, Phys. Rev. 120, 2041 (1960).
[27]J. Hubbard, Proc. Roy. Soc. (London) A276, 238 (1963); A277, 237 (1964).

PHYSICAL REVIEW B VOLUME 3, NUMBER 6 15 SEPTEMBER 1972

Diffusion of Mercury in Tin*

William K. Warburton†
Department of Physics, Harvard University, Cambridge, Massachusetts 02138
(Received 17 March 1972)

The diffusion rate of mercury was measured in the tin single crystals along both the a and c axes and is described by diffusion constants: $D_0^a = 30^{+20}_{-12}$ cm^2/sec, $D_0^c = 7.5^{+6.4}_{-3.5}$ cm^2/sec, $Q_D^a = 26.8 \pm 0.5$ kcal/mole, $Q_D^c = 25.3 \pm 0.6$ kcal/mole. This behavior does not differ greatly from the tin self-diffusion and in the light of present understanding of diffusion in polyvalent hosts, it seems most likely that the mercury is dissolved substitutionally and is diffusing by a vacancy mechanism. No good theoretical justification could be given to explain why mercury should prefer substitutional sites in tin, but be at least partially stable in interstitial-vacancy pairs in lead, although the possibility of van der Waals forces is discussed. Mercury diffusion is compared to diffusion of other impurities in tin and a new mechanism is suggested to explain the large anisotropy of diffusion of gold and silver between the tin a and c directions.

I. INTRODUCTION

In recent years diffusivity measurements have been made on a variety of impurities in polyvalent metals, including tin. From these measurements, it seems that gold,[1] silver,[1] copper,[2] and possibly zinc[3] diffuse interstitially in such systems. Since mercury has the same valence as zinc, but a different size and electronic structure, a measurement of its diffusivity might shed additional light on the relative importance of these factors in determining the stability of interstitial impurities. This research was undertaken in conjunction with an investigation of the diffusivity of mercury in lead[4] both because of the availability of the nuclide Hg^{203} and also to provide similar information about the solvent's role in determining the nature of the diffusing defect. The work was done with single crystals to simplify the interpretation of results.

II. EXPERIMENTAL DETAILS

Serial sectioning on a precision sliding microtome was used to determine the penetration profiles of Hg^{203} in oriented tin single crystals after constant-temperature anneals of known duration. The crystals were grown to the desired [001] and [110] orientations using Cominco 99.9999% tin and high-purity graphite boats. They were then cut to length on a Servomet spark cutter and etched to remove damaged material. Laue backreflection photographs